

International Journal of Emerging Electric Power Systems

Volume 8, Issue 5

2007

Article 2

A New Linear Fractional Transformation Based Approach to Power System Robustness Analysis

Rafael Castellanos Bustamante*

Arturo Roman Messina†

Carlos Juarez‡

*Electrical Research Institute of Mexico, rcb@iie.org.mx

†Cinvestav, aroman@gdl.cinvestav.mx

‡cjuarez@gdl.cinvestav.mx

A New Linear Fractional Transformation Based Approach to Power System Robustness Analysis

Rafael Castellanos Bustamante, Arturo Roman Messina, and Carlos Juarez

Abstract

Large power systems are highly complex systems that defy predictions with any degree of certainty. In this paper, an analytical framework for the assessment of small signal stability under operating uncertainty is presented.

A rigorous analysis framework for the description of uncertainty in operating conditions is suggested. Using structured singular value theory and optimization tools, techniques for robust stability analysis of complex power systems are then derived and a method to quantify the effect of parametric uncertainties on the stability of critical inter-area modes is presented. A computationally-efficient method for modeling parametric uncertainty based on linear fractional transformation (LFT) theory is investigated and tested. With this approach, it becomes possible to estimate the effects of variations in the parameters of major transmission resources on the nominal stability of critical inter-area modes.

The use of the analysis methods is demonstrated on two systems: i) a two-machine test system, and ii) a two-area, 11-bus, 4-machine test system.

KEYWORDS: structured singular value, robustness analysis, parametric uncertainty, small signal analysis

1. Introduction

In recent years there has been a growing interest in the small signal analysis for large scale systems governed by uncertain models. Advances in robust control theory, along with the application of optimization techniques are beginning to make feasible the analysis of robust stability problems using small-signal analysis software [1-4]. These methods provide worst-case estimates of critical operating conditions and can be used to identify key uncertainty sources as well as to quantify the effect of uncertainty in operating condition on critical inter-area modes.

Large scale simulation of uncertainties of operating conditions is a complex problem. Uncertainty in operating conditions arises from poor knowledge about expected planning and operating conditions, varying load levels, uncertainty in the topology of the system and the great complexity and uncertainty in the scheduling of energy transactions [5]. Furthermore, power system dynamic behavior is becoming more unpredictable and variable, often involving complex interactions among controllers [6].

Variations in operating conditions may result in system performance deterioration. As more complex devices are being developed and installed, utilities are becoming increasingly aware of the critical role of uncertainty in system design and operation. Models that do not consider the impacts of these uncertainties will not accurately model the accompanying climatic responses. Allowing for uncertainty in operating conditions, increases the decision-making process and may result in increased system reliability and a better utilization of control resources. The difficulty in obtaining a realistic uncertainty characterization usually leads to conservative designs and operation.

Conventionally, small signal stability studies are conducted by analyzing system behavior around an expected operating condition [7]. Since linearization is performed around a few selected operating conditions, these methods essentially provide local information. Furthermore, the models ignore sources of uncertainty such as variations in operating conditions and changes in system structure. To minimize the effects of these uncertainties, sequential studies have to be conducted for each base case condition and expected operating scenario. These approaches, however, are known to be conservative

There has been much work in recent years devoted towards the characterization and quantification of uncertainty. Several analytical studies have underlined the high degree of sensitivity of small signal model simulations to variations in operating conditions and system structure. An emerging method that has been successfully applied for the development of robustness analysis is the structure singular value introduced by Doyle et al. [8,9].

In this context, Djukanovic *et al.* used SSV theory to determine robust stability of power systems with respect to variations in operating conditions [3]. More recently, Castellanos *et al.* proposed a technique for robust stability analysis of large power systems using the structured singular value theory [4]. The suitability of this technique for the numerical treatment of uncertainty has been validated in the context of small-disturbance robust stability analysis of uncertain large-scale systems.

This paper continues this investigation to develop a novel approach to characterize uncertainty arising from variations in operating conditions. An analysis framework for the assessment of small signal stability under operating uncertainty that overcomes some of the limitations of the existing analysis methods is presented. Unlike conventional small-signal analysis tools that are based on a linearized model of the system, the new model introduces a framework for small signal analysis in which variations in system operating conditions are explicitly included and treated. The approach performs the computation of robust stability margins in a single step using an optimization technique and does not require trial and error and repeated calculations at various operating conditions required when using conventional methods. The proposed methodology integrates commercial software with robustness analysis in order to provide accurate characterization of small signal stability.

The use of the analysis methods is demonstrated on two systems i) a two-machine test system, and ii) a two-area, 11-bus, 4-machine test system. Conventional small signal stability studies are used as benchmarks for comparison of robustness analysis to conventional studies.

Several fruitful research directions are identified including the incorporation of model structure uncertainty in the analysis.

2. Parametric Uncertainty Model

The evaluation of uncertainty effects on system dynamic performance is emerging as an area of increasing importance in the analysis of stability and control of power systems. This section briefly reviews existing approaches to parametric uncertainty modeling. Emphasis is placed on the analysis of conservatism introduced by the methods.

The first step in generating an uncertain model for use in robustness analysis is to generate a linear fractional representation which spans the operating space of interest in the problem [8].

Consider a general uncertain system represented by the state-space realization

$$\dot{\mathbf{x}} = \mathbf{f}(\mathbf{x}, \mathbf{p}) \quad (1)$$

where \mathbf{x} is the n -dimensional state vector, and $\mathbf{p} = [p_1, p_2, \dots, p_m]^T$ is the vector of independent uncertain parameters which are assumed to vary within some practical limits $p_k^{\min} \leq p_k \leq p_k^{\max}$. Assume further that each entry of the state matrix can be defined by a polynomial function of the parameters vector \mathbf{p} . A problem of particular interest is that of determining if the linearized system (1) is robustly stable for all possible parameter variations. This is a problem that can be efficiently dealt with using robustness theory.

A key difficulty in the analysis of uncertain systems is that they are not in explicit state space for required for robust theory. This section describes the salient features of the methodology employed for generating state-space representations from the original nonlinear system (1).

2.1 Affine Parameter Dependent Representation: the Min-Max Approach

If a functional dependence of the \mathbf{A} -matrix on the parameter vector \mathbf{p} exists, then the effect of parameter variations can be determined analytically in the neighborhood of an operating condition.

Let the linear system representation be expressed in the form [10]

$$\dot{\mathbf{x}} = \mathbf{A}(\mathbf{p}) \mathbf{x} \quad (2)$$

in which the entries of the state space matrix depend on the parameter vector \mathbf{p} . Assuming further that each varying element, (i, j) , of the \mathbf{A} state-space matrix changes without certain bounds $a_{ij}^{\min} \leq a_{ij} \leq a_{ij}^{\max}$, with nominal values $\bar{a}_{ij} = (a_{ij}^{\min} + a_{ij}^{\max})/2$, and $a_{ij} \in \mathfrak{R}^n$.

The variation in the entries of the state-space matrices can be written as

$$a_{ij} = \bar{a}_{ij} (1 + r_{ij} \delta_{a_{ij}}) = a_{ij_o} + \alpha_{ij} \delta_{a_{ij}} \quad , \quad i, j = 1, \dots, n \quad (3)$$

where $r_{ij} = (a_{ij}^{\max} - a_{ij}^{\min}) / (a_{ij}^{\max} + a_{ij}^{\min})$, and the modulus of the uncertainties is supposed to be bounded as follows $|\delta_{a_{ij}}| \leq 1$; the scaling factor $\alpha_{ij} = (a_{ij}^{\max} - a_{ij}^{\min}) / 2$ gives a measure of the relative uncertainty in the parameter. As discussed in [10,11], the method is straightforward to implement, but it leads to some conservatism since possible joint parametric uncertainties are ignored.

Combining the individual changes in (3) yields, a rationally dependent model of the form

$$\mathbf{x} = \mathbf{A}(\mathbf{p})\mathbf{x} = \left[\mathbf{A}_o + \sum_{i=1}^{n_A} \delta_i \mathbf{A}_i \right] \mathbf{x} \quad (4)$$

where \mathbf{A}_o represents the nominal system, while matrices \mathbf{A}_i describe variations from the nominal system. Inherent to this approach is the assumption that parameter variations appear explicitly in the linear representation (2).

2.2 Sensitivity-Based Models

A second approach is to approximate the effect which the variations of the parameters have on the nominal plant model using a truncated Taylor's series. Assume to this end that the dependence of the varying \mathbf{A} -matrix elements on the set of independent uncertain parameters can be expressed as $a_{ij} = f_{ij}(p_1, p_2, \dots, p_m)$, where the nonlinear functions are to be determined. Expanding this function in a Taylor's series around a nominal value yields [12,15]

$$\mathbf{A}(\mathbf{p}) = \mathbf{A}_o + \left. \frac{\partial \mathbf{A}}{\partial p_k} \right|_{p_k^o} \Delta p_k + \left. \frac{\partial^2 \mathbf{A}}{\partial p_k^2} \right|_{p_k^o} \Delta p_k^2 + \dots \quad (5)$$

or, in component form,

$$a_{ij}^{\text{var}}(p_k) \approx a_{ij} \Big|_{p_k^o} + \left. \frac{\partial a_{ij}}{\partial p_k} \right|_{p_k^o} (p_k - p_k^o) + \left. \frac{\partial^2 a_{ij}}{\partial p_k^2} \right|_{p_k^o} (p_k - p_k^o)^2 + \dots \quad (6)$$

where the partial derivatives can be computed analytically or numerically using finite differences.

In practice, however, the general calculation of functional sensitivities relating the effects of the parameter p_k on the varying elements of the matrices \mathbf{A}_i may not be readily available. Further, due to the high dimensionality of the plant, the general calculation of analytical models may become prohibitive. This is especially true for system representations in which the parameter p_k does not appear in explicit form in the state matrix \mathbf{A} . Finally, models of the form (6) are only valid in a neighborhood around a particular linearization point. This limits their applicability to investigate robustness over large regions of the operating space.

In order to be more precise, let p_k be an uncertain parameter and let p_k^o be its nominal value. From our previous discussion, the parametric uncertainty can be expressed as a parameter set of the form

$$p_k = \bar{p}_k (1 + r_k \delta_k), k = 1, \dots, m \quad (7)$$

in which

$$\bar{p}_k = \frac{(p_k^{\min} + p_k^{\max})}{2}, r_k = \frac{p_k^{\max} - p_k^{\min}}{p_k^{\min} + p_k^{\max}}$$

where \bar{p}_k is the mean parametric value, and r_k is the relative uncertainty in the parameter. Substitution of the uncertain parameter variation (7) in (6) yields the np order polynomial approximation form

$$a_{ij}^{\text{var}}(p_1^o + \Delta p_1^o) = a_{ij_o} + a_{ij_1} \delta + a_{ij_2} \delta^2 + \dots + a_{ij_{np}} \delta^{np}, \quad i, j = 1, \dots, n \quad (8)$$

where the coefficients $a_{ij_o}, a_{ij_1}, a_{ij_2}, \dots, a_{ij_{np}}$ depend on the initial conditions, p_k^o and the average value \bar{p}_k [10]; np and n are the polynomial and the state matrix order, respectively.

Equation (8) can be reinterpreted in terms of the δ 's as

$$\mathbf{x} = \mathbf{A}(\mathbf{p})\mathbf{x} = \left[\mathbf{A}_o + \sum_{i=1}^{n_d} \delta^i \mathbf{A}_i \right] \mathbf{x}.$$

Variations to these approaches are described in [1,3,4]. This model avoids the need for explicit representation of the state matrix and may be used to study complex systems.

We emphasize that in interpreting parameter variations in the uncertainty framework two fundamental problems are involved: (a) identifying the varying elements of the \mathbf{A} -matrix affected by the change in the set of uncertain parameters, and (b) and introducing an uncertain representation of such a change in the nominal plant model. These two issues are treated separately below.

In what follows a new model is presented which explicitly accounts for uncertainty in operating conditions and reduces conservatism. Unlike existing approaches, this formulation is based on numerical rather than analytical approximations and allows the study of general models for which no information on the internal structure of the state matrix is available.

3. Numerical Least-Squares Approximations

3.1 Least-Squares Approximation to Parameter Determination

A key issue in deriving an appropriate uncertain system representation is allowing for the role of parameter variations whose exact values are unknown but which are known to lie between some minimum and maximum values. Given a nonlinear model (1), it is always possible to perform numerical linearization over several points in the expected range of operating conditions and /or over all combinations of the uncertain parameters. The parameter vector could represent different load levels, power flow or any other variation in operating condition.

Let $p_k = (p_{k1} \ p_{k2} \ \cdots \ p_{kN})$, where N is the number of operating conditions, be the grid of operating conditions for the k th varying parameter corresponding to particular values of the admissible range of parameter variations.

To calculate the dependency of the coefficients of the state matrix, \mathbf{A} , on the varying parameters, we sequentially perform numerical linearizations over the selected operating space. The resulting linear models form a multi-model state description

$$\dot{\mathbf{x}} = (\mathbf{A}_{k1} + \mathbf{A}_{k2} + \cdots + \mathbf{A}_{kN})\mathbf{x} \quad (9)$$

which satisfactorily approximates all linearizations of the linear model (1).

Based on the min-max formulation in section 2.2 we assume that the functional dependency of the \mathbf{A} -matrix elements can be approximated by the higher order polynomial approximation

$$a_{ij}(p_k^o + \Delta p_k^o) = f_{ij}(p_k) = \hat{a}_{ij_0} + \hat{a}_{ij_1} p_k + \hat{a}_{ij_2} p_k^2 + \dots + \hat{a}_{ij_{np}} p_k^{np} \quad (10)$$

for $i, j = 1, \dots, n$ where the \mathbf{A}_i represent linearization at the i th operating condition, r is the order of the polynomial approximation, and the polynomial coefficients p_k^j are expressible in terms of the uncertainty variations. More generally, we consider estimation of the parameters $\hat{a}_{ij_0}, \hat{a}_{ij_1}, \dots, \hat{a}_{ij_r}$ in the model (10) using least-squares optimization.

Figure 1 illustrates the nature of this approach.

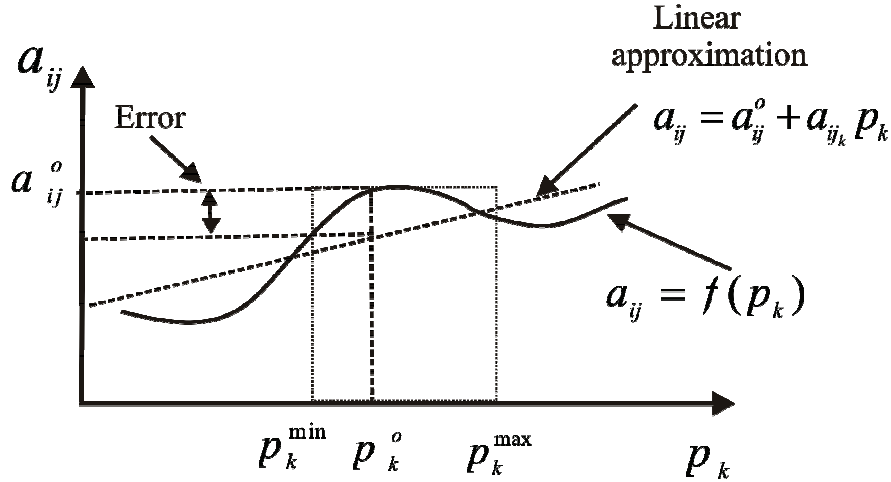


Figure 1. Functional dependency of the entries of the \mathbf{A} -matrix elements on variations in the k th system parameter

To illustrate the details of the proposed procedure consider the case of a single varying parameter, $\mathbf{p} = p_1$, which can be related to variations in the power system parameters such as loading or changes in tie-line structure. Let further the operating space be given by $p_1 = [p_{11} \ p_{12} \ \cdots \ p_{1N}]$, where N is the number of operating conditions considered in the analysis.

At each condition, the linear system representation becomes $\mathbf{x} = \mathbf{A}_l(p_1)\mathbf{x}$, $l = 1, \dots, N$. Note that since the parameter p_1 may not appear in explicit form in the state-matrix \mathbf{A}_l , a power flow solution is needed for each operating condition.

A critical issue in the application of the method is the identification of varying elements in the state-matrix representations. To determine significant deviations from the nominal value, we introduce the metric

$$d_i = |a_{i,j}^{\text{var}}(p_k^o + \Delta p_k)| = |a_{ij}^o - a_{ij}^o(p_k^o + \Delta p_k)| \quad (11)$$

where a_{ij}^o represents the nominal (unperturbed) condition. By neglecting terms with variations below a given threshold, the varying elements of the \mathbf{A} -matrix can be identified. Alternatively, numerical sensitivities can be computed.

For each varying element (a_{ij}^{var}) of the state matrix set, the coefficients in (10) can be determined using least-squares optimization. Application of this procedure to all operating conditions results in the set of (usually) over-determined equations

$$\begin{bmatrix} 1 & p_{11} & p_{11}^2 & \vdots & p_{11}^{np} \\ 1 & p_{12} & p_{12}^2 & \vdots & p_{12}^{np} \\ \vdots & \vdots & \vdots & \ddots & \vdots \\ 1 & p_{1N} & p_{1N}^2 & \vdots & p_{1N}^{np} \end{bmatrix} \begin{bmatrix} \hat{a}_{ij_0} \\ \hat{a}_{ij_1} \\ \hat{a}_{ij_2} \\ \vdots \\ \hat{a}_{ij_{np}} \end{bmatrix} = \begin{bmatrix} a_{ij_{Ak1}} \\ a_{ij_{Ak2}} \\ \vdots \\ a_{ij_{AkN}} \end{bmatrix} \quad (12)$$

where the coefficients $a_{ij_{kl}}$ are the (i, j) varying entries of the \mathbf{A} state matrices which change respect to the nominal condition, i.e. $(\mathbf{A}_{nom} - \mathbf{A}_{kl})$.

Equivalently, the system (12) can be written in compact form as

$$\mathbf{X} \mathbf{a}_{ij}^{\text{var}} = \mathbf{y} \quad (13)$$

where

$$\mathbf{a}_{ij}^{\text{var}} = [\hat{a}_{ij_0} \ \hat{a}_{ij_1} \ \hat{a}_{ij_2} \ \cdots \ \hat{a}_{ij_{np}}]^T; \quad \mathbf{y} = [a_{ij_{Ak1}} \ a_{ij_{Ak2}} \ \cdots \ a_{ij_{AkN}}]^T$$

$$\mathbf{X} = \begin{bmatrix} 1 & p_{11} & p_{11}^2 & \vdots & p_{11}^{np} \\ 1 & p_{12} & p_{12}^2 & \vdots & p_{12}^{np} \\ \vdots & \vdots & \vdots & \ddots & \vdots \\ 1 & p_{1N} & p_{1N}^2 & \vdots & p_{1N}^{np} \end{bmatrix}$$

The solution of the unknown vector $\mathbf{a}_{ij}^{\text{var}} = [\hat{a}_{ij_0} \ \hat{a}_{ij_1} \ \hat{a}_{ij_2} \ \cdots \ \hat{a}_{ij_{np}}]^T$ is then obtained using a least-squares solution $\mathbf{a}_{ij}^{\text{var}} = (\mathbf{X}^T \mathbf{X})^{-1} \mathbf{X} \mathbf{y}$. Techniques to solve (13) are described in [4] and are not repeated here.

Several issues arise in the practical implementation of the method:

- (1). The selection of the optimal order of the polynomial approximation (np)
- (2). The determination of the number of operating conditions (N)
- (3). The computation of the coefficients $\hat{a}_{ij_0}, \hat{a}_{ij_1}, \hat{a}_{ij_2}^2, \dots, \hat{a}_{ij_{np}}^{np}$
- (4). The identification of the varying entries (a_{ij}^{var}) of the linearized power system representations

Experience with the analysis of large-scale uncertain systems [4] suggests that a second-order polynomial approximation and three operating conditions suffice to accurately determine stability margins. With these simplifications, the least-squares optimization reduces to the conventional problem

$$\begin{bmatrix} \hat{a}_{i,j_0} \\ \hat{a}_{i,j_1} \\ \hat{a}_{i,j_2} \end{bmatrix} = \begin{bmatrix} 1 & p_{11} & p_{11}^2 \\ 1 & p_{12} & p_{12}^2 \\ 1 & p_{13} & p_{13}^2 \end{bmatrix}^{-1} \begin{bmatrix} a_{i,j_{A_1}} \\ a_{i,j_{A_2}} \\ a_{i,j_{A_3}} \end{bmatrix} \quad (14)$$

This speed ups computations and enables the efficient determination of robust stability margins.

3.2 Linear Fractional Representation

The cornerstone to this whole procedure is the estimation of an accurate representation of the system. Once the coefficients of the polynomial formulation are obtained, the variations in the coefficients of the \mathbf{A} -matrix coefficients can be obtained. Substituting $P_1 = p_a + p_b \delta$ into (10), the uncertain plant with structured uncertainty becomes,

$$a_{ij}^{\text{var}} = a_{ij_0} + a_{ij_1} \delta_1 + a_{ij_2} \delta_1^2 \quad (15)$$

$$\begin{aligned} a_{ij_0} &= \hat{a}_{ij_0} + \hat{a}_{ij_1} p_a + \hat{a}_{ij_2} p_a^2 \\ a_{ij_1} &= [\hat{a}_{ij_1} + 2\hat{a}_{ij_2} p_a] p_b \\ a_{i,j_2} &= \hat{a}_{ij_2} p_b^2 \\ p_a &= \frac{P_{\max} + P_{\min}}{2}, \quad p_b = \frac{P_{\max} - P_{\min}}{2} \end{aligned}$$

Repeating the same procedure for each varying element, we obtain the perturbed system

$$\dot{\mathbf{x}} = \mathbf{A}(\mathbf{p})\mathbf{x} = (\mathbf{A}_o + \Delta\mathbf{A})\mathbf{x} = [\mathbf{A}_o^{\text{var}} + \mathbf{A}_1^{\text{var}}(\delta_1\mathbf{I}) + \mathbf{A}_{11}^{\text{var}}(\delta_1^2\mathbf{I})]\mathbf{x} \quad (16)$$

where the polynomial coefficients $a_{ij_0}, a_{ij_1}, a_{ij_2}$ are the i,j th entries of matrices $\mathbf{A}_o^{\text{var}}, \mathbf{A}_1^{\text{var}}, \mathbf{A}_{11}^{\text{var}}$, respectively. Matrix $\mathbf{A}_o^{\text{var}}$ represents the nominal plant. Observe

that $\mathbf{A}_1^{\text{var}} = \mathbf{A}_{11}^{\text{var}} = 0$ yields the nominal model of the power system and matrices $\mathbf{A}_x^{\text{var}}$ contain the coefficients of the polynomial functions.

A similar result holds for higher order system approximations.

The closed-loop system is then formed by connecting the uncertainty representation to the nominal model.

Following Morton and McAfoos [12], we define a linear system with fictitious inputs and outputs

$$\begin{bmatrix} \dot{\mathbf{x}} \\ \mathbf{x} \\ z_1 \\ z_2 \\ \vdots \\ z_n \end{bmatrix} = \begin{bmatrix} \mathbf{A}_o & \mathbf{E}_1 & \mathbf{E}_2 & \cdots & \mathbf{E}_n \\ \mathbf{G}_1 & 0 & 0 & 0 & 0 \\ \mathbf{G}_2 & 0 & 0 & 0 & 0 \\ \vdots & 0 & 0 & 0 & \mathbf{0} \\ \mathbf{G}_n & 0 & 0 & 0 & 0 \end{bmatrix} \begin{bmatrix} \mathbf{x} \\ w_1 \\ w_2 \\ \vdots \\ w_n \end{bmatrix} \quad (17)$$

Computation of the interconnected uncertainty system representation for the augmented plant is then straightforward. To convert the system into the standard form for μ analysis, we define the matrices

$$\mathbf{M}_{11} = \mathbf{A}_o^{\text{var}} \quad ; \quad \mathbf{M}_{12} = [\mathbf{I} \ \mathbf{0} \ \mathbf{I} \ \mathbf{0}]$$

$$\mathbf{M}_{21} = \begin{bmatrix} \mathbf{A}_1^{\text{var}} \\ \mathbf{I} \\ \mathbf{A}_2^{\text{var}} \\ \mathbf{I} \end{bmatrix} \quad ; \quad \mathbf{M}_{22} = \begin{bmatrix} 0 & \mathbf{A}_{11}^{\text{var}} & 0 & \mathbf{A}_{12}^{\text{var}} \\ 0 & 0 & 0 & 0 \\ 0 & 0 & 0 & \mathbf{A}_{22}^{\text{var}} \\ 0 & 0 & 0 & 0 \end{bmatrix}$$

The LFT of the uncertain system given by these expressions can then be easily cast into the following state-space form

$$\begin{bmatrix} \dot{\mathbf{x}} \\ \mathbf{z} \end{bmatrix} = \begin{bmatrix} \mathbf{M}_{11} & \mathbf{M}_{12} \\ \mathbf{M}_{21} & \mathbf{M}_{22} \end{bmatrix} \begin{bmatrix} \mathbf{x} \\ \mathbf{w} \end{bmatrix} \quad (18)$$

and

$$\mathbf{w} = \Delta \mathbf{z} \quad (19)$$

where $\Delta(\delta)$ has the diagonal structure $\Delta(\delta) = \text{blockdiag}(\delta_1 I \ \delta_2 I)$. Here \mathbf{M}

represents the known part of the system, and Δ represents the uncertainty present in the system.

Figure 2 shows the general framework for robust stability analysis used in the analysis. It can be seen that the relationship between the input and the output signal of the closed-loop system is given by the upper linear fractional transformation (LFT)

$$F_u(\mathbf{M}, \Delta(\delta)) = \mathbf{M}_{22} + \mathbf{M}_{21} \Delta(\delta) (\mathbf{I} - \mathbf{M}_{11} \Delta(\delta))^{-1} \mathbf{M}_{12} \quad (20)$$

Once we have the LFT-based uncertainty description, robustness can be assessed using μ analysis. Let $\Delta(s)$ represent the set of allowable varying conditions represented as uncertainties. Referring to Fig. 1, it can be shown [8] that the perturbed closed-loop system is stable for all $\Delta(s)$ with $\|\Delta(j\omega)\|_\infty \leq 1$ if and only if $\mathbf{M}(s)$ is stable (i.e. $\mathbf{M}(s)$ has all of its poles in the open left-half plane and $F_u(\mathbf{M}, \Delta(\delta))$ remains in an H_∞ norm sense bounded by unity, that is if and only if

$$\max \mu_\Delta(\mathbf{M}_{22} + \mathbf{M}_{21} (I - \Delta \mathbf{M}_{11})^{-1} \Delta \mathbf{M}_{12}) < 1 \quad \forall \omega, \|\Delta\|_\infty \leq 1 \quad (21)$$

where μ_Δ denotes the structured singular value, and $\|\cdot\|_\infty$ is the infinity norm. If this condition is satisfied, the system is said to be robustly stable, i.e. if the system is stable for all permissible Δ 's.

A value of $\mu_\Delta < 1$ implies that no perturbation within Δ exists that will destabilize the feedback system. Alternatively, this condition can also be interpreted as saying that the true plant dynamics are stable, assuming these dynamics lie within the range generated by the nominal model dynamics coupled with the set of modeling errors.

Finally, small signal stability margins can be determined using (21). The procedure described above is quite straightforward and general.

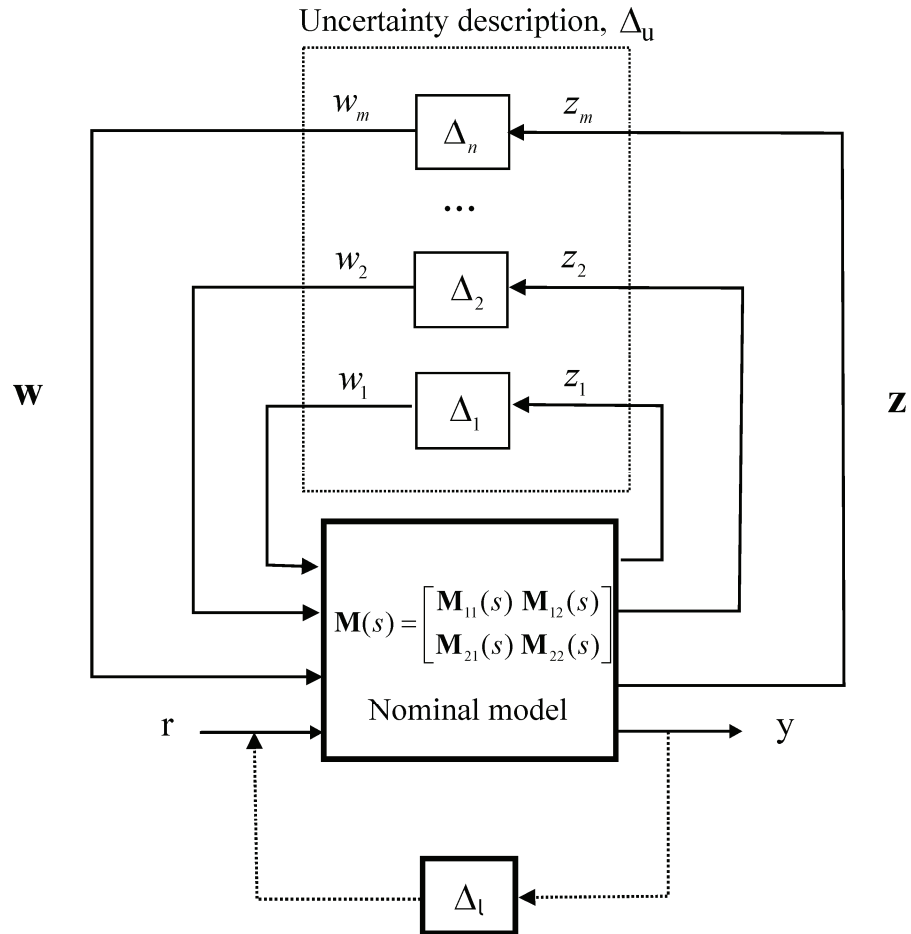


Figure 2. Feedback loop with structured perturbation

4. Numerical Results

In order to illustrate the accuracy and performance of the present method, two test cases were considered, namely, a single-machine infinite bus, and a two-area test system. In both cases, the analytical predictions were compared with results from conventional eigen-analysis using a commercial small-signal stability program and Prony analysis.

The uncertainty scenarios included:

- Parametric uncertainty involving variations in generation levels, and
- Combined uncertainty in both operating conditions and uncertainty in the topology of the system arising from contingency conditions

The following sections describe the uncertainty definition for each case.

4.1 Single-Machine Infinite Bus System

As a first example of the application of the technique we analyze a single-machine infinite bus system shown in Figure 3. The transmission system consists of two parallel ac lines and a local load.

The transmission lines have a reactance of 0.5 p.u y 0.95 p.u., respectively, and the transformer reactance is 0.15 p.u. on a base of 2200 MVA. The load is 450+j300 MW. Figure 3 gives the power flows for the nominal operating condition.

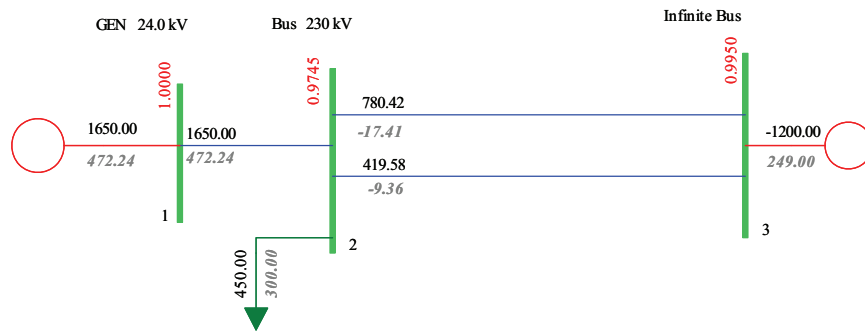


Figure 3. On line diagrams of the single-machine infinite bus test system.

The generator is round rotor with d and q axis transient and subtransient effects represented, and equipped with a fast excitation system. The local static load is represented as constant impedance for both active and reactive power; the overall state system has 10 states. Appendix A provides dynamic data used in the simulations.

The procedure outlined in section 3 was then applied to generate an uncertain model of the system. Two sources of uncertainty in operating conditions are considered and investigated; uncertainty in transmission power flows, and uncertainty in the interconnecting tie-line reactance.

4.1.1 Single Varying Parameter

In this case, the generated power is modeled as a structured uncertainty. Following the approach in section 3, the operating space was approximated by three operating points representing different levels of power generation, namely $\mathbf{p}_1 = [1550 \text{ MW} \quad 1650 \text{ MW} \quad 1700 \text{ MW}]$. At each operating condition a load flow simulation is performed and the associated linearized model was derived. For instance, \mathbf{A}^{1650} represents the state matrix related to the operating condition with a generated power of 1650 MW.

The base model used in the studies is a 10-state linearization of the nonlinear system model at each operating points; the states of the model are $\delta, \Delta\omega_r, E'_d, E'_q, E''_d, E''_q, X_{e_1}, X_{e_2}, X_{e_3}$ and X_{e_4} . The nominal model corresponds to a 1650 MW intertie power transfer.

As a benchmark for comparison against the proposed technique, linear models were obtained using SSAT [14]. In this analysis, the generated power was increased in small steps until instability was detected. Any increase in generation is compensated by the infinite bus.

Stressing the system by increasing the generated power, the oscillatory mode becomes unstable when the generated power is about 1700 MW. Table 1 depicts the damping and frequency of the critical electromechanical mode as a function of generated power.

Table 1
Damping of critical mode as a function of generated power.

Generated Power (MW)	Eigenvalue	Damping ratio (%)	Frequency (Hz)
1550	-0.0853± j7.4849	1.14	1.91
1650	-0.0252± j7.4094	0.34	1.80
1700	0.0067± j7.3682	- 0.09	1.73

Based on the chosen admissible uncertainty, an uncertain model was developed. In order to identify the coefficients of the state matrices that change with the operating condition, we use the metric $d_i = \mathbf{A}_i^{dif} = (\mathbf{A}^{nom} - \mathbf{A}^{\#nom})$ where $\mathbf{A}^{nom} = \mathbf{A}^{1650}$ represents the linearized model for a 1650 MW power transfer.

For the one uncertain parameter case we can define \mathbf{A}_I^{dif} and \mathbf{A}_{II}^{dif} as the varying matrices obtained from the differences $\mathbf{A}_I^{dif} = (\mathbf{A}^{1650} - \mathbf{A}^{1550})$ and $\mathbf{A}_{II}^{dif} = (\mathbf{A}^{1650} - \mathbf{A}^{1700})$, respectively. For the case under study, \mathbf{A}_I^{dif} has ten varying entries with magnitudes larger than the adopted criterion, ε whilst \mathbf{A}_{II}^{dif} has eight varying entries. Matrix \mathbf{A}_I^{dif} was chosen for robust stability assessment in the following studies.

The \mathbf{A}_I^{dif} matrix has the general structure

$$\mathbf{A}_I^{dif} = \begin{bmatrix} 0 & a_{12} & a_{13} & a_{14} & a_{15} & a_{16} & 0 & 0 & 0 & a_{110} \\ 0 & 0 & 0 & 0 & 0 & 0 & 0 & 0 & 0 & 0 \\ 0 & 0 & 0 & 0 & 0 & 0 & 0 & 0 & 0 & 0 \\ 0 & a_{42} & 0 & 0 & 0 & 0 & 0 & 0 & 0 & a_{410} \\ 0 & 0 & 0 & 0 & 0 & 0 & 0 & 0 & 0 & 0 \\ 0 & a_{62} & 0 & 0 & 0 & 0 & 0 & 0 & 0 & a_{610} \\ 0 & 0 & 0 & 0 & 0 & 0 & 0 & 0 & 0 & 0 \\ 0 & 0 & 0 & 0 & 0 & 0 & 0 & 0 & 0 & 0 \\ 0 & 0 & 0 & 0 & 0 & 0 & 0 & 0 & 0 & 0 \\ 0 & 0 & 0 & 0 & 0 & 0 & 0 & 0 & 0 & 0 \end{bmatrix}$$

while the corresponding entries of the state matrices which change with the operating conditions are:

$$\Delta \mathbf{A}^{1550 MW} = \begin{bmatrix} 0 & -70.43 & -33.35 & -32.08 & -3.76 & -28.66 & 0 & 0 & 0 & 70.43 \\ 0 & 0 & 0 & 0 & 0 & 0 & 0 & 0 & 0 & 0 \\ 0 & 0 & 0 & 0 & 0 & 0 & 0 & 0 & 0 & 0 \\ 0 & -5.95 & 0 & 0 & 0 & 0 & 0 & 0 & 0 & 5.95 \\ 0 & 0 & 0 & 0 & 0 & 0 & 0 & 0 & 0 & 0 \\ 0 & -4.94 & 0 & 0 & 0 & 0 & 0 & 0 & 0 & 4.94 \\ 0 & 0 & 0 & 0 & 0 & 0 & 0 & 0 & 0 & 0 \\ 0 & 0 & 0 & 0 & 0 & 0 & 0 & 0 & 0 & 0 \\ 0 & 0 & 0 & 0 & 0 & 0 & 0 & 0 & 0 & 0 \\ 0 & 0 & 0 & 0 & 0 & 0 & 0 & 0 & 0 & 0 \end{bmatrix}$$

$$\Delta \mathbf{A}^{1650 MW} = \begin{bmatrix} 0 & -69.62 & -34.12 & -33.82 & -3.44 & -26.16 & 0 & 0 & 0 & 69.62 \\ 0 & 0 & 0 & 0 & 0 & 0 & 0 & 0 & 0 & 0 \\ 0 & 0 & 0 & 0 & 0 & 0 & 0 & 0 & 0 & 0 \\ 0 & -6.10 & 0 & 0 & 0 & 0 & 0 & 0 & 0 & 6.10 \\ 0 & 0 & 0 & 0 & 0 & 0 & 0 & 0 & 0 & 0 \\ 0 & -4.56 & 0 & 0 & 0 & 0 & 0 & 0 & 0 & 4.56 \\ 0 & 0 & 0 & 0 & 0 & 0 & 0 & 0 & 0 & 0 \\ 0 & 0 & 0 & 0 & 0 & 0 & 0 & 0 & 0 & 0 \\ 0 & 0 & 0 & 0 & 0 & 0 & 0 & 0 & 0 & 0 \\ 0 & 0 & 0 & 0 & 0 & 0 & 0 & 0 & 0 & 0 \end{bmatrix}$$

$$\Delta \mathbf{A}^{1700 MW} = \begin{bmatrix} 0 & -69.18 & -34.47 & -33.15 & -3.28 & -24.94 & 0 & 0 & 0 & 69.18 \\ 0 & 0 & 0 & 0 & 0 & 0 & 0 & 0 & 0 & 0 \\ 0 & 0 & 0 & 0 & 0 & 0 & 0 & 0 & 0 & 0 \\ 0 & -6.16 & 0 & 0 & 0 & 0 & 0 & 0 & 0 & 6.16 \\ 0 & 0 & 0 & 0 & 0 & 0 & 0 & 0 & 0 & 0 \\ 0 & -4.37 & 0 & 0 & 0 & 0 & 0 & 0 & 0 & 4.37 \\ 0 & 0 & 0 & 0 & 0 & 0 & 0 & 0 & 0 & 0 \\ 0 & 0 & 0 & 0 & 0 & 0 & 0 & 0 & 0 & 0 \\ 0 & 0 & 0 & 0 & 0 & 0 & 0 & 0 & 0 & 0 \\ 0 & 0 & 0 & 0 & 0 & 0 & 0 & 0 & 0 & 0 \end{bmatrix}$$

Having identified the varying entries associated with the set of state matrices the coefficients of the quadratic approximation for each varying element ij are determined by solving a least-squares problem (refer to Eq. (14)). More precisely, the coefficients associated with the varying entry a_{12} are obtained from

$$\begin{bmatrix} a_{120} \\ a_{121} \\ a_{122} \end{bmatrix} = \begin{bmatrix} 1 & 1550 & 1550^2 \\ 1 & 1650 & 1650^2 \\ 1 & 1700 & 1700^2 \end{bmatrix}^{-1} \begin{bmatrix} -70.43 \\ -69.62 \\ -69.18 \end{bmatrix}$$

where

$$a_{120} = -75.349,$$

$$a_{121} = -0.0015,$$

$$a_{122} = 0.3042 \times 10^{-5}$$

The analysis above suggests that we can express the variations in the terms of the \mathbf{A} -matrix which vary with the generation change in an analytical form. These results indicate that over the range of variations of interest, the variation in the

coefficient a_{12} can be sufficiently accurately approximated by a second order polynomial representation of the form

$$a_{12} = a_{12_0} + a_{12_1}P_1 + a_{12_2}P_1^2 = -75.35 - 0.0015P_1 + 0.304 \times 10^{-5}P_1^2$$

Repeating the least-squares fit for each varying element of matrix \mathbf{A}_I^{dif} we obtain the following uncertain matrices $\mathbf{A}_0^{var}, \mathbf{A}_1^{var}, \mathbf{A}_{11}^{var}$ that contain the effects of the polynomial function coefficients.

$$\mathbf{A}_0^{var} = \begin{bmatrix} 0 & -75.349 & -9.356 & -9.00 & -10.067 & -76.654 & 0 & 0 & 0 & 72.284 \\ 0 & 0 & 0 & 0 & 0 & 0 & 0 & 0 & 0 & 0 \\ 0 & -1.244 & 0 & 0 & 0 & 0 & 0 & 0 & 0 & 1.239 \\ 0 & 0 & 0 & 0 & 0 & 0 & 0 & 0 & 0 & 0 \\ 0 & -12.206 & 0 & 0 & 0 & 0 & 0 & 0 & 0 & 12.202 \\ 0 & 0 & 0 & 0 & 0 & 0 & 0 & 0 & 0 & 0 \\ 0 & 0 & 0 & 0 & 0 & 0 & 0 & 0 & 0 & 0 \\ 0 & 0 & 0 & 0 & 0 & 0 & 0 & 0 & 0 & 0 \\ 0 & 0 & 0 & 0 & 0 & 0 & 0 & 0 & 0 & 0 \\ 0 & 0 & 0 & 0 & 0 & 0 & 0 & 0 & 0 & 0 \end{bmatrix}$$

$$\mathbf{A}_1^{var} = \begin{bmatrix} 0 & -0.0015 & -0.0228 & -0.0219 & 0.0048 & 0.0365 & 0 & 0 & 0 & 0.0016 \\ 0 & 0 & 0 & 0 & 0 & 0 & 0 & 0 & 0 & 0 \\ 0 & -0.0045 & 0 & 0 & 0 & 0 & 0 & 0 & 0 & 0.0045 \\ 0 & 0 & 0 & 0 & 0 & 0 & 0 & 0 & 0 & 0 \\ 0 & 0.0055 & 0 & 0 & 0 & 0 & 0 & 0 & 0 & -0.0055 \\ 0 & 0 & 0 & 0 & 0 & 0 & 0 & 0 & 0 & 0 \\ 0 & 0 & 0 & 0 & 0 & 0 & 0 & 0 & 0 & 0 \\ 0 & 0 & 0 & 0 & 0 & 0 & 0 & 0 & 0 & 0 \\ 0 & 0 & 0 & 0 & 0 & 0 & 0 & 0 & 0 & 0 \\ 0 & 0 & 0 & 0 & 0 & 0 & 0 & 0 & 0 & 0 \end{bmatrix}$$

$$\mathbf{A}_{11}^{\text{var}} = 1 \times 10^{-5} \begin{bmatrix} 0 & \mathbf{0.3042} & 0.4717 & 0.4536 & -0.0473 & -0.3601 & 0 & 0 & 0 & -0.3069 \\ 0 & 0 & 0 & 0 & 0 & 0 & 0 & 0 & 0 & 0 \\ 0 & 0.0942 & 0 & 0 & 0 & 0 & 0 & 0 & 0 & -0.0944 \\ 0 & 0 & 0 & 0 & 0 & 0 & 0 & 0 & 0 & 0 \\ 0 & -0.0513 & 0 & 0 & 0 & 0 & 0 & 0 & 0 & 0.0511 \\ 0 & 0 & 0 & 0 & 0 & 0 & 0 & 0 & 0 & 0 \\ 0 & 0 & 0 & 0 & 0 & 0 & 0 & 0 & 0 & 0 \\ 0 & 0 & 0 & 0 & 0 & 0 & 0 & 0 & 0 & 0 \\ 0 & 0 & 0 & 0 & 0 & 0 & 0 & 0 & 0 & 0 \\ 0 & 0 & 0 & 0 & 0 & 0 & 0 & 0 & 0 & 0 \end{bmatrix}$$

Substituting $P_1 = p_a + p_b \delta$ defined in (15) into (10) and using the procedure explained in section (3.1), the uncertain plant with structured uncertainty becomes

$$\mathbf{A} = \mathbf{A}_o + \mathbf{A}_1(\delta_1 \mathbf{I}) + \mathbf{A}_{11}(\delta_1^2 \mathbf{I})$$

Based on the preceding small-signal results, the ability of the technique for assessing robust stability was considered. The μ plot in figure 4 shows a peak value of $\mu = 1.26$ which indicates that the system is robustly unstable ($\mu > 1$) for this range of operating conditions.

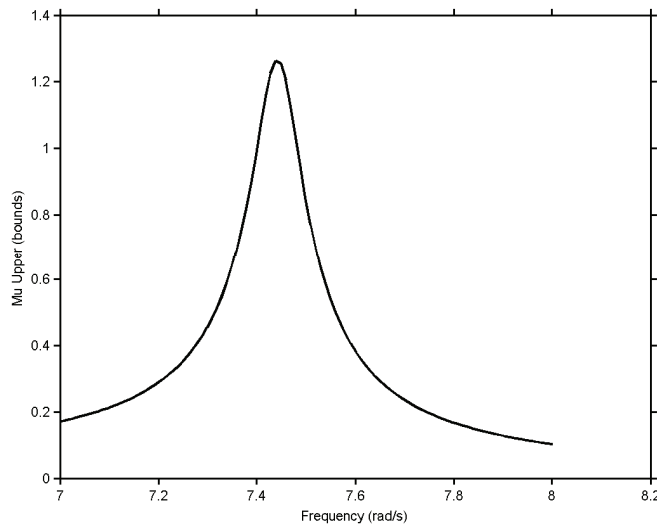


Figure 4. Robust stability μ plot

The largest range of generation power for which the system is guaranteed to remain stable can then be approximated by

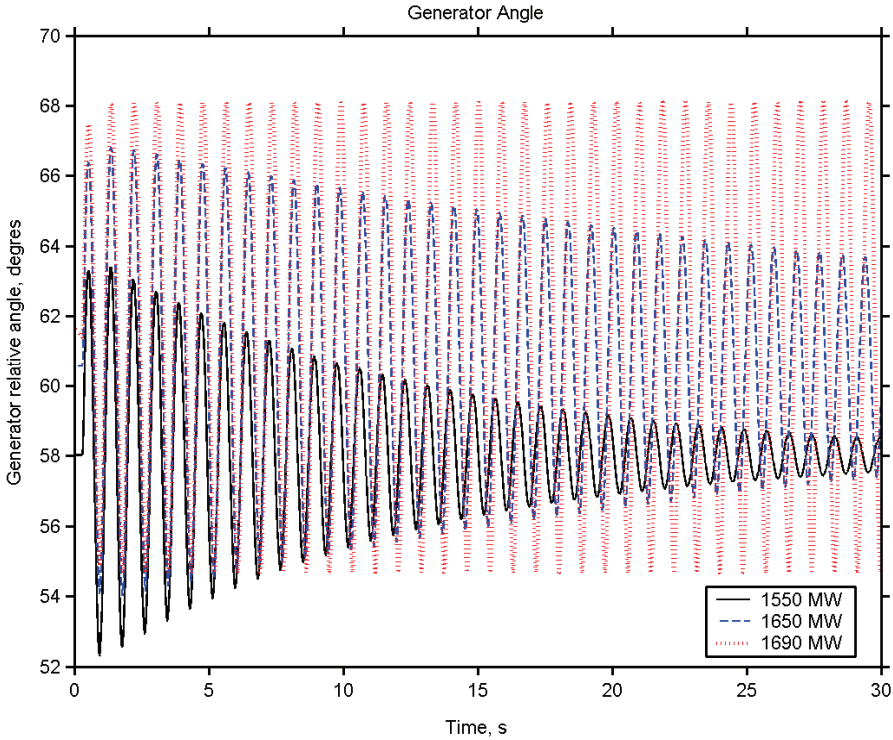
$$\text{estimated generated power} = \frac{P_{\max} + P_{\min}}{2} + \frac{P_{\max} - P_{\min}}{2} \delta = 1685 \text{ MW}$$

where $\delta = 1/\mu$. The corresponding estimated oscillation frequency is 7.44 rad/s (1.18 Hz) which closely corresponds to the linear analysis results in Table 1. Results determined from robustness analyses are found to be in excellent agreement with those of conventional eigenanalysis. Comparison of the error between the exact value in Table 1 (1690 MW) and the estimated generated power using robust analysis is of about 1.95% which indicates that the robust stability procedure is accurate.

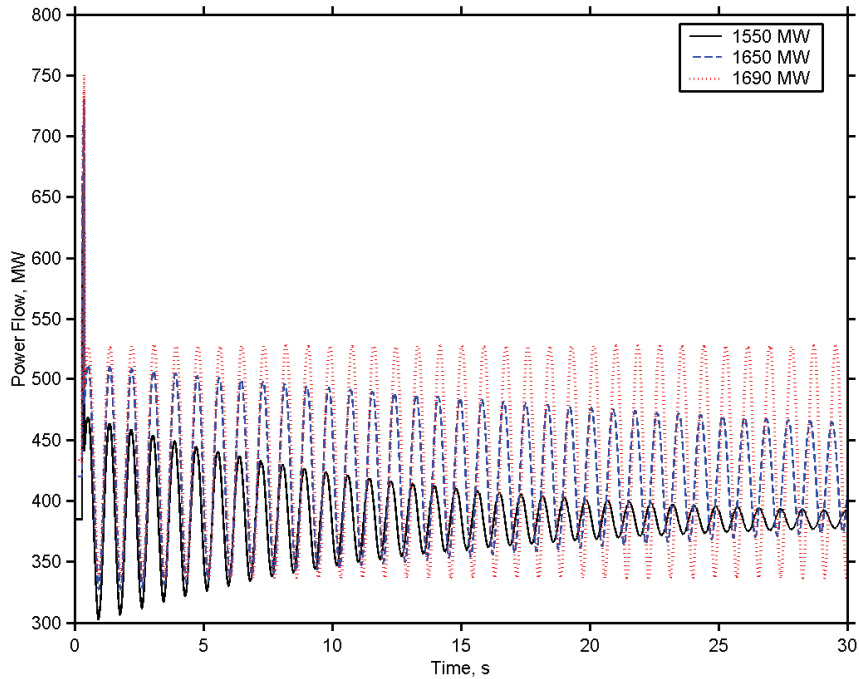
Although more operating conditions could be used to improve these results, experience with the study of large uncertain power system models shows that those used here are sufficient to produce an accurate system representation for the analysis of practical systems [4].

4.1.2 Prony Analysis on Tansient Stability Output Data

Prony analysis was used to further confirm robustness findings. The simulated contingency is the outage without fault of transmission line #1. The line was reconnected after 5 cycles. Figure 5 shows the dynamic behavior of selected signals for various levels of tie-line power.



a) Generator relative angle



b) Power Flow on circuit one of line Bus two- Infinite Bus

Figure 5. Several system parameters for three generated powers on synchronous machine.

Note that in this case the system becomes unstable for an intertie power flow of about 1690 MW in good agreement with analytical predictions. Table 2 compares the identified damping ratio and frequency of the system mode for various levels of power transfers. These results are again in good agreement with robust stability analysis results.

Table 2
Prony results

Generated Power (MW)	Real part (1/s)	Imaginary part (rad/s)	Frequency (Hz)	Damping ratio (%)
1550	-0.085	7.45	1.190	1.139
1650	-0.025	7.40	1.177	0.338
1690	0.000	7.36	1.171	0.000

4.1.3 Two Varying Parameters Case, p_1, p_2

A second major source of uncertainty in power operation derives from variations in the interconnecting tie-line reactance, $X_{tie-line}$. In this section, both the interconnecting reactance and the generation level are used to simultaneously assess the influence of uncertainty of operating conditions on the nominal stability of the system mode. In this study, the interconnecting tie-line reactance was varied from the nominal condition with the transmission lines in service, to a stressed system conditions with one of the circuits out of services.

To compute the critical loading condition, the system was stressed by increasing the MW transfer to the infinite bus. To increase the MW transfer, the generation was increased gradually and this load increase was met by an equal amount of generation decrease in the infinite bus.

The robust stability analysis procedures indicated in section 3 were used to represent $X_{tie-line}$ and the generation level as structured uncertainties. The analysis of upper bounds in figure 6 shows a peak bigger than one suggests that the system is unstable. Table 3 shows the estimated and exact equivalent reactance and generated power along with the eigenvalue calculated at the estimated parameters. The absolute error between the exact and estimated parameters is 2.32% and 0.12% for $X_{tie-line}$ and generated power, respectively.

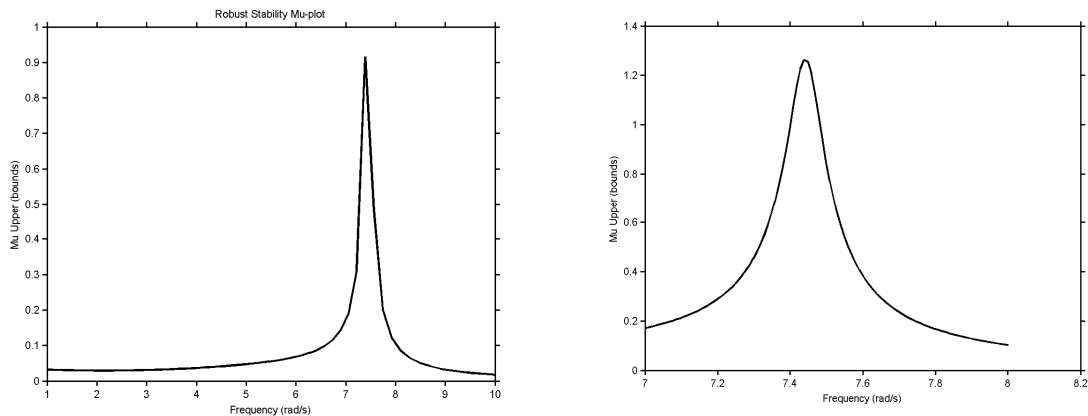


Figure 6. Robust stability μ plot. a) Frequency sweep from 0 to 10 rad/s; b) Frequency sweep around the critical frequency (7.3 rad/s).

Table 3
Robust stability analysis results

μ upper bounds	24.56
Estimated ω (rad/s)	7.4111
Exact ω (rad/s)	7.3334
Estimated $X_{tie-line}$ (p.u.)	0.3321
Exact $X_{tie-line}$ (p.u.)	0.3400
Error (%)	2.32
Estimated power flow (MW)	1628.1
Exact power flow (MW)	1630
Error (%)	0.12
Exact eigenvalue	$-0.0005 \pm j7.3334$
	$\zeta = 0.01 \%$

4.2 Two-Area Test System

As a second example we consider a 2-area, 4-machine test system from Ref. [15]. Figure 7 shows a single-line diagram of this system. The transmission system consists of 9 buses, 4 generators, 8 lines, 4 transformers and 2 loads. In addition, shunt compensators and a static VAR compensator are used to support system voltage. The state space model of the system has 48 states.

The dynamic characteristics of this system are strongly dependent on system structure and the amount of power transfer over the major intertie. Network robustness is also of importance as the loss of a transmission circuits leads to reduced small-signal stability margins.

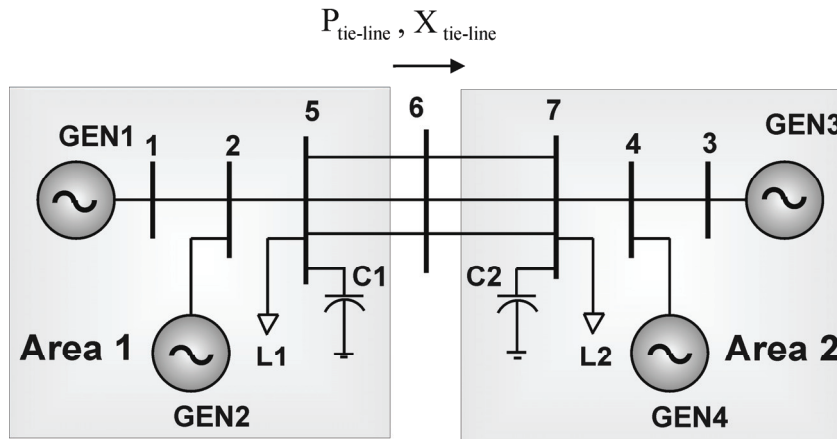


Figure 7. Two-area power system

For the purposes of this study, machines all generators are represented using detailed subtransient models and fast static excitation models (refer to Appendix). A SVC, with supplementary damping control, was installed at the midpoint of the intertie. The load model used is constant current for the real component and constant impedance for the reactive component.

The effectiveness of the proposed technique is demonstrated through two case studies. In the first case study, the power transfer between Areas 1 and 2, $P_{tie-line}$, is modeled as a varying, uncertain parameter. In the second case, the interconnecting tie-line reactance, $X_{tie-line}$, is considered as an uncertain quantity. We finally examine the application of the developed procedures to determine the worst-case operating conditions as well as to analyze uncertainties occurring simultaneously at several locations in the system.

Small signal stability studies were performed to assess system stability margins when subjected to small variations in operating conditions, as well as to benchmark the robust stability analysis results.

Eigenvalue analysis of this system identifies three electromechanical modes of concern which are shown in Table 4. The study focuses on the effects of varying levels of power transfers on the stability of the inter-area mode.

Table 4
Electromechanical system eigenvalues

Mode description	Real part (1/s)	Imaginary part (rad/s)	Frequency (Hz)	Oscillation mode pattern
Inter-area	-0.321	4.037	0.64	GEN1,GEN2 vs GEN3,GEN4
Local 1	-0.463	6.863	1.09	GEN1 vs GEN2
Local 2	-1.227	7.559	1.20	GEN3 vs GEN4

For robust stability analysis, a grid of operating conditions is determined from a parameter space of the form

$$P_{tie-line} = [p_{11} \ p_{12} \ p_{13}]$$

$$X_{tie-line} = [X_{11} \ X_{12} \ X_{13}]$$

Here, the first value for the interconnecting reactance corresponds to the normal operating condition with all circuits in service, whilst the second and third values, correspond to the case with one and two circuits out of service. This is a highly complex case since the conventional determination of critical parameter values requires a large number of simulations to estimate the stability limits.

A systematic analysis of these uncertainties was performed to determine their impact on the stability of the inter-area modes using the LFT-based framework. In this procedure the uncertainty in model parameters was represented by specifying

a grid of six operating conditions. This model was found to give an accurate enough approximation to the parameter space.

From the μ plot in figure 8, we can see that, for the limiting condition, μ has a dominant frequency at about 0.64 Hz (3.22 rad/s) larger than one suggesting that the system is robustly unstable.

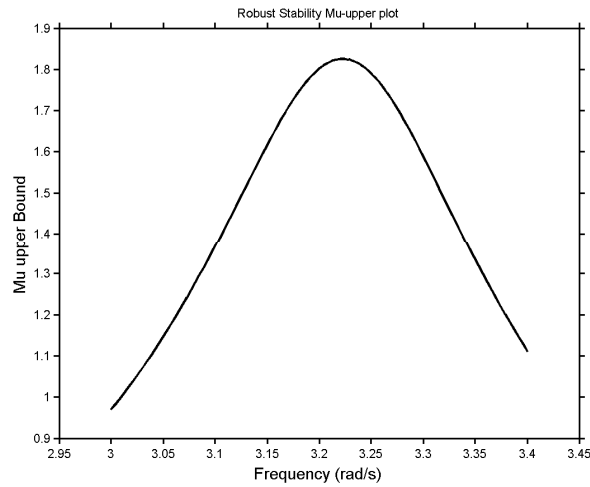


Figure 8. Robust stability μ plot for two varying parameters

Table 5 shows the estimated and exact equivalent reactance and power flow along with the eigenvalue calculated at the exact instability condition determined using conventional eigenanalysis. As can be seen Table 5, the errors between the exact and estimated parameters are -7.6% and -1.41% for $X_{tie-line}$ and $P_{tie-line}$, respectively.

Table 5
Robust stability analysis results - Two varying parameters case

μ upper bounds	1.8247
Estimated ω (rad/s)	3.2248
Exact ω (rad/s)	2.1798
Estimated $X_{tie-line}$ (p.u.)	0.1868
Exact $X_{tie-line}$ (p.u.)	0.2010
Error (%)	-7.6
Estimated power flow (MW)	417.8
Exact power flow (MW)	423.7
Error (%)	-1.41
Exact eigenvalue	$0.0077 \pm j2.1798$
	$\zeta = -0.35\%$

It can be seen that uncertainty analysis gives a good prediction of the highest limiting power transfer. The results for the limiting reactance, on the other hand, are deemed satisfactory considering the range of variation in operating conditions considered in the study.

5. Conclusion

In this paper, an LFT-based uncertainty description of structured, real uncertainty arising from variations in operating conditions has been proposed. Other classes of uncertainties can also be treated, provided that they do not modify the dimension of the state representation. The mathematical framework permits consideration of complex systems and provides an accurate representation of uncertainty of the model over a wide range of parameter variations.

The methodology can open many doors for investigators to allow more natural, uncertainty modelling in power system studies. In addition, this approach can greatly facilitate solution of robust stability, particularly for real-time, and/or large scale applications.

These tools are being integrated into management and operational planning tools using commercial small signal stability software.

Appendix A. Single-machine infinite-bus system data-PTI format

```
1 'GENROU' G1 8.0 0.03 1.0 0.07 3.50 0.0 1.81 1.76 0.30 0.65 0.23 0.15
0.0 0.0 /
3 'GENCLS' G3 99999.0 0.0 /
1 'SEXS' G1 0.1 0.1 85. 0.1 0 3/
```

Appendix B. Two-Area System Dynamic Data (PTI format)

```
1 'GENROU' 1      8.0      0.03      0.4      0.05      6.5      0.0
1.8      1.7      0.3      0.55      0.25      0.2      0.0392      0.267 /
1 'EXAC4' 1      0.01      0.5      -0.5      0.0      0.0      200      0.0      7.0      -7.0      0.0 /
1 'ESDC2A' 1      0.05      20      0.055      0.0      0.0      3.5      -0.06
1.46      0.36      0.125      1.8      0.0      0.4      1.2      0.2      0.0 /
1 'STAB1' 1      20      10      2.5      0.02      0.556      5.4      0.2 /
```

References

- [1] Badri Ramanathan, Vijay Vittal, "Small-disturbance angle stability enhancement through direct load control Part I – framework development", *IEEE Trans. on Power Systems*, vol. 21, no. 2, pp. 773-781, May 2006.
- [2] Miodrag Djukanovic, Mustafa Khammash, and Vijay Vittal, "Application of the Structured Singular Value Theory for Robust Stability and Control Analysis in Multimachine Power Systems", Parts I and II. *IEEE Trans. on Power Systems*, vol. 13, no. 4, pp. 1311-1316, 1998.
- [3] Miodrag B. Djukanovic, Mustafa H. Khammash, and Vijay Vittal, "Sensitivity based structured singular value approach to stability robustness of power systems", *IEEE Trans. on Power Systems*, vol. 15, no. 2, May 2000, pp. 825-830.
- [4] R. Castellanos, A. R. Messina, H. Sarmiento, "Robust stability analysis of large power systems using the structured singular value theory", *International Journal of Electrical Power and Energy Systems*, vol. 27, issues 5-6, July 2005, pp 389-397.
- [5] M. Ivey, A. Akhil, D. Robinson, J. Stamp, K. Stamber, and K. Chu, "Accommodating Uncertainty in the Planning and Operations of Electric Power Systems", Sandia Report SAND2000-1681, Sandia National Laboratories, July 2000.
- [6] John F. Hauer, "Robust damping control for large power systems", *IEEE Control Systems Magazine*, vol. 9, no. 1, Jan. 1989, pp. 12-18.
- [7] Cigre Task Force 07, Study Committee 38, "Analysis and Control of Power System Oscillations, Final Report, 1996.
- [8] J. Doyle, "Analysis of feedback systems with structured uncertainties", *IEE Proceedings*, Part D, vol. 129, no. 6, pp. 242-250, November 1982.
- [9] A. Packard, and J. C. Doyle, "The complex structured singular value", *Automatica*, vol. 29, no. 1, pp. 71-109, 1993.
- [10] A. Varga, G. Looye, D. Moormann and G. Grubel " Automated Generation of LFT_Based Parametric Uncertainty Descriptions from Generic Aircraft Models", *Mathematical and Computer Modelling of Dynamical Systems*, 1998, Vol. 4, Num. 4, pp. 249-274.
- [11] Thomas Mannchen, Klaus H. Well, "Uncertainty bands approach to LFT modeling", *Lectures Notes in Control and Information Sciences, Advanced Techniques for Clearance of Flight Control Laws*, vol. 283, 2002, pp. 211-220.
- [12] B. Morton, and A. McAfoos, "A μ test for real parameter variations" *Proceedings of the American Control Conference*, pp. 135-138, 1985.
- [13] G.J. Balas, J.C. Doyle, K. Glover, A. Packard, R. Smith, " μ -Analysis and Synthesis Toolbox, Matlab" MUSYN Inc. and The MathWorks, Inc. V. 3.05 (Release 12), January 2001.

- [14] Powertech Labs Inc. "Small Signal Analysis Tool, SSAT", Version 2.1, 2002.
- [15] P. Kundur, Power System Stability and Control The EPRI Power Engineering Series, New York: McGraw-Hill, Inc., 1994.